

**An Investigation of the Resistance Rise and Power Fade
in High-Power Li-ion Cells***

Ira Bloom, Scott A. Jones, Vincent S. Battaglia,
Edward G. Polzin, and Gary L. Henriksen
Electrochemical Technology Program
Argonne National Laboratory
9700 South Cass Avenue
Argonne, IL 60439

Chester G. Motloch, Jon P. Christophersen, Jeffrey R. Belt,
Chinh D. Ho, and Randy B. Wright
Idaho National Engineering and Environmental Laboratory
P.O. Box 1625
Idaho Falls, ID 83415

Rudolph G. Jungst, Herbert L. Case, and Daniel H. Doughty
Sandia National Laboratories
P.O. Box 5800
Albuquerque, NM 87185

To be presented at the:
19th Seminar & Exhibit on Primary & Secondary Batteries
Fort Lauderdale, FL
March 11-14, 2002

The submitted manuscript has been created by the University of Chicago as Operator of Argonne National Laboratory ("Argonne") under Contract No. W-31-109-ENG-38 with the U.S. Department of Energy. The U.S. Government retains for itself, and others acting on its behalf, a paid-up, nonexclusive, irrevocable worldwide license in said article to reproduce, prepare derivative works, distribute copies to the public, and perform publicly and display publicly, by or on behalf of the Government.

*This research was performed under the auspices of the U.S. Department of Energy, under Contract No. W-31-109-ENG-38.

An Investigation of the Resistance Rise and Power Fade in High-Power Li-ion Cells

Ira Bloom, Scott A. Jones, Vincent S. Battaglia, Edward G. Polzin and Gary L. Henriksen
Electrochemical Technology Program
Argonne National Laboratory
9700 South Cass Avenue
Argonne, IL 60439

Chester G. Motloch, Jon P. Christophersen, Jeffrey R. Belt,
Chinh D. Ho and Randy B. Wright
Idaho National Engineering and Environmental Laboratory
P.O. Box 1625
Idaho Falls, ID 83415

Rudolph G. Jungst, Herbert L. Case, and Daniel H. Doughty
Sandia National Laboratories
P.O. Box 5800
Albuquerque, NM 87185

Abstract

Two different cell chemistries, Gen 1 and Gen 2, were subjected to accelerated aging experiments. In Gen 1 calendar-life experiments, useful cell life was strongly affected by temperature and time. Higher temperatures accelerated the degradation of cell performance. The rates of resistance increase and power fade followed simple laws based on a power of time and Arrhenius kinetics. The data have been modeled using these two concepts, and the calculated data agree well with the experimental values.

The Gen 1 calendar-life resistance increase and power fade data follow $(\text{time})^{1/2}$ kinetics. This may be due to solid electrolyte interface (SEI) layer growth. From the cycle-life experiments, the resistance increase data also follow $(\text{time})^{1/2}$ kinetics. But there is an apparent change in overall power fade mechanism going from 3% to 6% ΔSOC . Here, the power of time changes to a value less than 0.5, indicating that the power fade mechanism is more complex than layer growth.

The Gen 2 calendar- and cycle-life experiments show the effect of cell chemistry on kinetics. The calendar-life resistance and power fade follow either linear or linear plus $(\text{time})^{1/2}$ kinetics, depending on temperature. Temperature dependence for the kinetic law was also found in the cycle-life data. At 25°C, the resistance increase (and power fade) follows linear kinetics, while at 45°C, $(\text{time})^{1/2}$ kinetics are found.

1. Introduction

The U.S. Department of Energy established the Advanced Technology Development (ATD) Program to address key issues limiting the life and safety of high-

power Li-ion batteries. In this program, three national laboratories- Argonne National Laboratory (ANL), Idaho National Engineering and Environmental Laboratory (INEEL), and Sandia National Laboratories (SNL), are working develop an understanding of the effect of accelerated calendar- and cycle-life testing on the performance of Li-ion cells, especially on the resistance and power of the cells.

This experimental effort used two different Li-ion cell chemistries in 18650-size packages. The cells were built to ANL’s specifications. The Gen 1 cells used the best commercially available cell chemistry at the time of construction. The Gen 2 cells used materials that were either developed in the ATD Program or selected based on extensive screening of the most advanced materials that could be obtained worldwide.

The Gen 1 calendar and cycle life experiments used a complete factorial matrix. Using the results from the Gen 1 cells, we were able to model the changes in resistance and power with time. The modeling helped elucidate the types of fade mechanisms present. The Gen 2 experiments were much more limited. Using just three temperatures, we were able to learn much about the degradation processes at work and how they are affected by cell chemistry.

2. Experimental

The experimental conditions and results for the Gen 1 work have been presented elsewhere [1]. Briefly, the exact compositions of the Gen 1 and Gen 2 cells are given in Tables 1 and 2, respectively.

Table 1. Gen 1 Cell Chemistry

Positive Electrode	Negative Electrode
8 wt% PVDF binder 4 wt% SFG-6 graphite 4 wt% carbon black 84 wt% $\text{LiNi}_{0.8}\text{Co}_{0.2}\text{O}_2$	9 wt% PVDF binder 16 wt% SFG-6 graphite 75 wt% MCMB-6 graphite
Electrolyte	Separator
1M LiPF_6 in EC/DEC (1:1 by wt)	37- μm thick PE Celgard separator

The cathodes and anodes were cast as thin films on aluminum and copper foils, respectively, to yield an effective active area of 678 cm^2 . After assembly, the cells underwent a few formation cycles and a 21-day stand before shipping to the test labs.

Table 2. Gen 2 Cell Chemistry

Positive Electrode	Negative Electrode
8 wt% PVDF binder 4 wt% SFG-6 graphite 4 wt% carbon black 84 wt% $\text{LiNi}_{0.8}\text{Co}_{0.15}\text{Al}_{0.05}\text{O}_2$	8 wt% PVDF binder 92 wt% MAG-10 graphite
Electrolyte	Separator
1.2 M LiPF_6 in EC/EMC (3:7 by wt)	25- μm thick PE Celgard separator

The cathodes and anodes were cast as thin films on aluminum and copper foils, respectively, to yield an effective active area of $\sim 846 \text{ cm}^2$.

In the Gen 1 aging studies, three to six cells were used at each condition. The calendar-life study using the Gen 1 cells was a complete factorial matrix that consisted of four temperatures (40, 50, 60, and 70°C) and three states of charge (SOC, 40, 60 and 80%). These SOCs correspond to open-circuit voltages (OCVs) of 3.600, 3.747 and 3.918 V, respectively. Additional information was gathered during the soak periods at temperature. Because of different equipment at the three test labs, two types of calendar-life tests were performed. ANL measured the leakage current (Group A). SNL and INEEL conducted the pulse-per-day calendar test (Group B) [2].

The cycle-life study using the Gen 1 cells was also a complete factorial matrix. In addition to the parameters mentioned for the calendar-life work, three ΔSOCs (3 and 6%, given in Figs. 1 and 2) were used [2].

The calendar-life study using the Gen 2 cells was more limited. It consisted of aging the cells at 45 and 55°C and 60% SOC (3.761 V). The pulse-per-day calendar test was used at ANL. The cycle-life study consisted of aging the cells at 45 and 25°C using a scaled 25-Wh PNGV profile [3] at INEEL.

For both Gen 1 and Gen 2, each cell was characterized, by the hybrid pulse power characterization test (HPPC) [4] and other tests. After four weeks at the desired temperature (two weeks for the cells at 70°C), changes in cell performance were gauged by cooling the cells down and repeating the HPPC test at 25°C . For Gen 1 and Gen 2 cells, power change was determined at 60% SOC.

Cell end-of-life was performance-based. If the cell could not perform the 6th HPPC pulse within its voltage window, the cell had reached the end-of-life criterion.

A detailed analysis of the HPPC data in deriving the resistance and power is given in references 1, 4, and 5, and will not be given here. All further analyses focused on changes in discharge resistance and power.

The derived values at 60% SOC were pooled and averaged. They were used in curve fitting experiments to elucidate temperature and time dependencies. The Gen 1 cell data could be fit to the general equation

$$Q = A \exp(-E_a/RT) t^z \quad (1)$$

where Q is the resistance or power change; A the pre-exponential factor; E_a the activation energy in J; R , the gas constant; T the absolute temperature, t , time; and z , the exponent of time. This equation was linearized by taking the natural logarithm of both sides of the equation and using the Microsoft EXCEL function LINEST to calculate $\ln A$, E_a/R , and z . In addition, LINEST returned the standard error (S.E.) around each parameter and the regression coefficient, r^2 .

No temperature dependency was calculated from the Gen 2 data, since only two temperatures were used for each aging condition. The data were curve fit using the general expression

$$Q = f(t), \quad (2)$$

where $f(t)$ is $at + b$, or $at^{1/2} + b$ (a and b are constants) or a linear combination of them, and monitoring r^2 .

3. Results and Discussion

For clarity, the results and discussion for Gen 1 and Gen 2 are presented separately.

Gen 1. In general, the cells at higher temperatures reached end of life before the ones at lower temperatures. For example, in both the calendar- and cycle-life tests, the 70°C cells failed after two weeks of testing. The ones at 60°C tended to fail after four weeks of testing. In addition to the temperature effect on life, cycling the cells and pulsing them during the calendar test tended to shorten their lives. Premature cell failure and cell leakage produced a sparse data matrix to analyze. The initial average values for the cell populations are given in Table 3. The average error around these values is 5 to 7%.

Table 3. Initial Average Values from Cells in This Study

Test / Group	Resistance, mΩ	Power, W
80% calendar life	73.3	43.83
60% calendar life (A)	65.9	45.95
60% calendar life (B)	73.9	30.12
40% calendar life	66.8	46.36
Cycle life (all SOCs and ΔSOCs)	59.1	36.11

Note: 80, 60 and 40% indicate the SOC. (A) indicates cells monitored for leakage current. (B) indicates cells subject to one current pulse a day.

Calendar Life. Typical resistance-versus-SOC (as given by the cell voltage, 60% = 3.747 V OCV) and power-versus-SOC curves are given in Figs. 3 and 4. The curves in these figures show the expected trends: resistance increases with time and power decreases with time.

The parameters from all of the fits are given in Table 4 for the three SOCs. The cells exposed to 70°C and 80% SOC failed very quickly. Very little resistance and power data were obtained under these conditions; these cells were excluded from further analysis. Table 4 also contains the fitting results using the remaining temperature data at 40, 50, and 60°C. From the values of r^2 , most of the fits are very good and the data followed square-root-of-time (sqrt) and Arrhenius kinetics.

Table 4. Resistance Change and Power Fade Fitting Parameters

%SOC		Resistance Increase				Power Fade			
		z	E_a/R , K	$\ln A$	r^2	z	E_a/R , K	$\ln A$	r^2
40	Value	0.52	6827.30	23.1	0.98	0.44	6095.95	20.83	0.97
	S.E.	0.05	350.94	1.04		0.06	423.05	1.25	
60/A	Value	0.51	6810.67	23.49	0.99	0.46	5541.28	19.36	0.81
	S.E.	0.06	374.31	1.11		0.18	1086.14	3.21	
60/B	S.E.	0.51	4828.96	17.50	0.94	0.41	3820.41	14.31	0.93
	S.E.	0.16	759.73	2.18		0.13	636.16	1.83	
80	Value	0.61	2715.18	10.74	0.87	0.46	2262.09	9.47	0.83
	S.E.	0.14	719.42	2.18		0.15	750.39	2.27	

Plots containing example resistance and power changes are given in Figs. 5 and 6. In these plots, markers represent the experimental values and the calculated values are represented by curves.

The fact that both resistance and power change with $(\text{time})^{1/2}$ implies that the data follow either one-dimensional kinetics or some other mechanism that has $(\text{time})^{1/2}$

dependency. In the literature, the kinetics of thin-film growth have been described as having $(\text{time})^{1/2}$ dependence. Applying these concepts to the lithium-ion battery, growth of a thin-film, solid electrolyte interface (SEI) layer may be the cause of the observation [6,7]. Based on the data from this study, we do not know on which electrode the SEI layer is growing. However, based on literature reports [8], we think it is the SEI layer on the cathode that makes the largest contribution to the observed changes.

Cycle Life. The plots of resistance and power versus cell voltage are very similar to those shown in Figs. 3 and 4, respectively. Indeed, the trends in the resistance increase and power fade are analogous.

The fitting parameters for the SOC_s and Δ SOC_s are given in Table 5. From these data, the value of z in Eq. (1) for the resistance at a given SOC is strongly dependent on the Δ SOC. At 60% SOC and 3% Δ SOC, the z value is approximately 0.50; while at 6% Δ SOC, it is approximately 0.10. In the case of power fade, at 60% SOC, there is also a marked change in mechanism going from 3% to 6% Δ SOC, as indicated by the values of z . The situation at 80% SOC is not as clear-cut. The values of z at 3% and 6% Δ SOC, 0.19 and 0.14, respectively, are not statistically different from one another, and, hence, may be the same.

As discussed in the calendar-life section, a z value of 0.5 may indicate one-dimensional diffusion kinetics or to SEI layer growth. The lower values of z indicate that a different mechanism than film growth proportional to film thickness is causing resistance increases. Possible alternative mechanisms coming into play are the dissolution of the SEI with time, a separate reaction of the PVDF binder with the electrodes, or the reaction of LiPF₆ with the electrodes and/or electrolyte [9].

Table 5. Fitting Parameters from Cycle Life Study

SOC, %	Δ SOC,%		Resistance Increase				Power Fade			
			z	E_a/R , K	$\ln A$	r^2	z	E_a/R , K	$\ln A$	r^2
60	3	Value	0.54	3414.94	13.52	0.98	0.25	2079.32	9.49	1.00
		S.E.	0.09	368.24	1.03		0.00	1.99	0.01	
	6	V	0.11	1881.29	9.48	0.94	0.08	1330.07	7.46	0.92
		S.E.	0.08	378.44	1.09		0.07	306.43	0.89	
80	3	V	0.57	4648.37	17.19	0.96	0.19	2940.95	12.17	0.99
		S.E.	0.12	566.63	1.63		0.14	396.34	1.09	
	6	V	0.15	2317.42	10.84	0.91	0.14	1739.50	8.74	0.91
		S.E.	0.10	487.42	1.40		0.07	341.04	0.98	

Gen 2. These cells had a significantly better performance and longer life than those of Gen 1. The initial average values from the HPPC test for resistance and power were 32.7 m Ω and 67.7 W, respectively, as opposed to those of Gen 1 cells given in

Table 3. In our analysis of the HPPC data, some distinct differences in dependence on time were seen.

Calendar Life. Plots of discharge resistance and power fade versus time are given in Figs. 7 and 8, respectively. These plots show the data from the experiments at 45 and 55°C. Allowing for some scatter, these data seem to be nearly linear with time.

Indeed, fitting a straight line to the data in Fig. 7 yields r^2 values of 0.98 and 0.87 for 55°C and 45°C, respectively. The corresponding r^2 values for the data in Fig. 8 are 0.95 and 0.77. A linear-with-time kinetic law seems to describe the 55°C data well, but not the 45°C data. A closer examination of the 45°C data reveals that there are actually two regions, one early in cell life that is linear with time and the other later in cell life that is proportional to (time)^{1/2}. This is shown in Fig. 9 along with the values of r^2 . A better kinetic law for these data is of the form, resistance = $at + bt^{1/2}$, where a and b are constants and t is time. Performing a least-squares fit using this equation yields a value of r^2 of 0.95. The same time dependencies were found for the 45°C data shown in Fig. 8.

In the literature, the growth of a thin film, (e.g., a SEI layer,) can be proportional to (time)^{1/2}. Square-root-of-time-dependent (parabolic kinetics), as well as linear-with-time, mechanisms have been found for the growth of an oxide film on a metal surface [10–15]. The square-root-of-time-dependent mechanisms tend to have a strong thermal diffusion component and follow Arrhenius kinetics. In the linear-with-time case, the rate of oxidation is constant with time, and is thus independent of the amount of gas or metal previously consumed in the formation of the oxide layer. The linear growth law is found to describe metal oxidation reactions whose rate is controlled by a surface reaction step or by diffusion of one of the reactants to the surface of the metal.

Applying this analogy to the Li-ion battery case, the formation of a thin film on a Li-ion battery electrode may occur in much the same manner as an oxide film on a metal. It is possible that the reaction of the electrolyte with an electrode to form species, such as lithium alkoxides, lithium carbonates, or LiF, follows parabolic kinetics. For linear kinetics, the diffusion of LiPF₆ with its electrolyte solvent cage to the electrode may be linear with time.

Cycle Life. A plot of the increase in discharge resistance with time is given in Fig. 10 for the two temperatures, 25 and 45°C. It shows that the mechanism of resistance increase is very sensitive to temperature. The resistance increase at 25°C is linear with time, while that at 45°C depends on (time)^{1/2}. The power fade follows an analogous pattern.

As discussed in the calendar-life section under Gen 2, there are many possible mechanisms for the resistance increase. Which exact mechanism is in operation depends on temperature, test conditions, and cell chemistry. The delineation of the exact mechanism or mechanisms is the subject of intense research.

Conclusions

In Gen 1 calendar-life experiments, useful cell life was strongly affected by temperature and time. Increased temperature accelerated cell performance degradation. The rates of resistance increase and power fade followed simple laws based on a power-of-test-time and Arrhenius kinetics. The data have been modeled using these two concepts and the calculated data agree well with the experimental values.

The Gen 1 calendar life resistance increase and power fade data follow $(\text{time})^{1/2}$ kinetics. This may be due to SEI layer growth. From the cycle-life experiments, the resistance increase data also follow $(\text{time})^{1/2}$ kinetics. But there is an apparent change in the overall power fade mechanism going from 3% to 6% ΔSOC . Here, the power of time changes to a value less than 1/2 indicating that the power fade mechanism is more complex than SEI layer growth.

The Gen 2 calendar-life resistance and power fade follow either linear or linear plus $(\text{time})^{1/2}$ kinetics, depending on temperature. Temperature dependence for the kinetic law was also found in the cycle-life data. At 25°C, resistance increase (and power fade) follows linear kinetics, while at 45°C, $(\text{time})^{1/2}$ kinetics are found.

Acknowledgement

This work was performed under the auspices of the U.S. Department of Energy, Office of Advanced Automotive Technologies, under Contract No. W-31-109-Eng-38.

References

1. I. Bloom, B. W. Cole, J. J. Sohn, S. A. Jones, E. G. Polzin, V. S. Battaglia, G. L. Henriksen, C. Motloch, R. Richardson, T. Unkelhaeuser and H. L. Case, *J. Power Sources* **101** (2001) 238–247.
2. C. G. Motloch, I. Bloom, T. Unkelhaeuser, *Gen 1: Cell Development and Testing; Overview of ATD Gen 1 Cell Performance and Life Evaluations*, USDOE OAAT FY 2000 Progress Report for the Advanced Technology Development Program, December 2000.
3. C. Motloch, J. Christophersen, R. Wright, R. Richardson, C. Ho, D. Glenn, K. Gering, T. Murphy, I. Bloom, S. Jones, V. Battaglia, G. Henriksen, R. Jungst, H. Case, T. Unkelhaeuser, and D. Doughty, *Overview of ATD Gen 2 Cell Performance and Life Evaluations*, USDOE OAAT FY 2001 Progress Report for the Advanced Technology Development Program
4. PNGV Battery Test Manual, DOE/ID-10597, Rev. 3, February 2001.
5. R. A. Sutula et al., FY 2000 Progress Report for the Advanced Technology Development Program, U.S. DOE, OAAT, December 2000.
6. E. Strauss, D. Golodnitsky, and E. Peled, *Electrochemical and Solid State Letters*, **2** (1999) 115-117.
7. G. Blomgren, *J. Power Sources*, **81-82** (1999) 112-118.

8. K. Amine, M. J. Hammond, J. Liu, C. Chen, D. W. Dees, A. N. Jansen, and G. L. Henriksen, Proc. of the 10th Int. Meeting on Lithium Batteries, Como, Italy, May 28-June 2, 2000, p. 332.
9. See E. Peled, D. Golodnitsky, C. Menachem, and D. Bar-Tow, *J. Electrochem. Soc.*, **145**, (1998) 3482–3486 for a more complete discussion of the types of reactions that can occur in a lithium-ion battery.
10. N. Birks and G. H. Meier, Introduction to High Temperature Oxidation of Metals, Edward Arnold Ltd., London, 1983.
11. Per Kofstad, High-Temperature Oxidation of Metals, John Wiley and Sons, New York, 1966.
12. K. Hauffe, Oxidation of Metals, Plenum Press, New York, 1965.
13. W. Jost, Diffusion in Solids, Liquids and Gases, 3rd Printing, Addendum, Academic Press, Inc., New York, 1960.
14. J. Crank, The Mathematics of Diffusion, 2nd edition, Clarendon Press, Oxford, 1975.
15. Per Kofstad, Nonstoichiometry, Diffusion, and Electrical Conductivity in Binary Metal Oxides, John Wiley and Sons, New York, 1972.

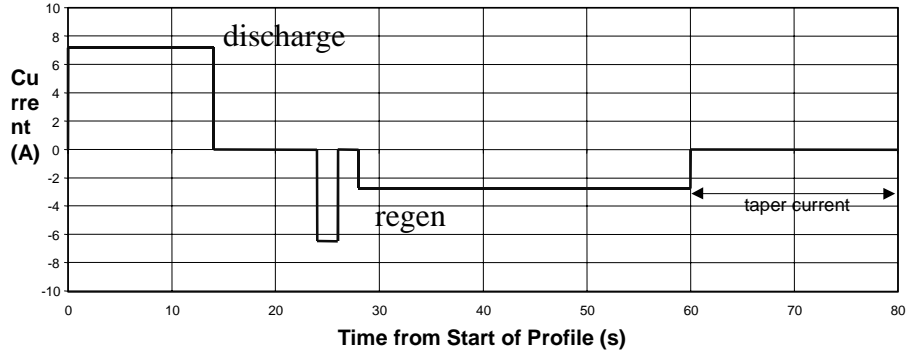


FIG. 1. Profile for 3% Δ SOC.

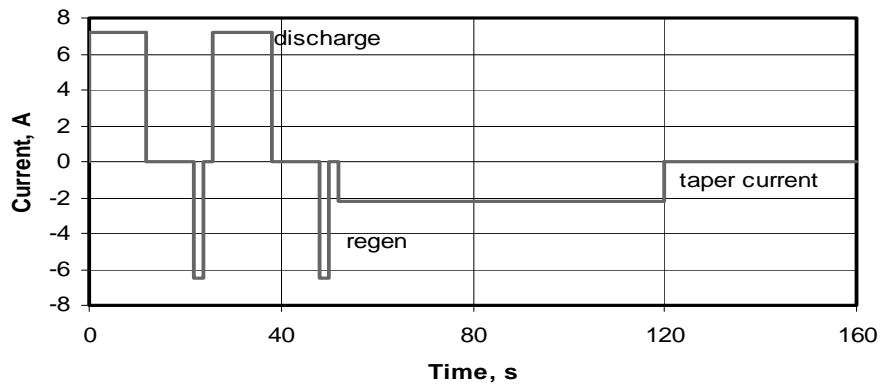


FIG. 2. Profile for 6% Δ SOC.

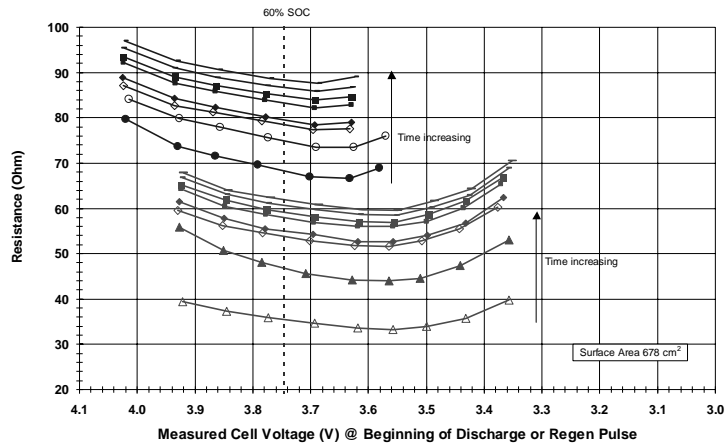


FIG. 3. Typical HPPC-derived resistance vs. cell voltage data. The top set of curves are from discharge and the bottom, from regen. These curves represent data spanning 28 weeks.

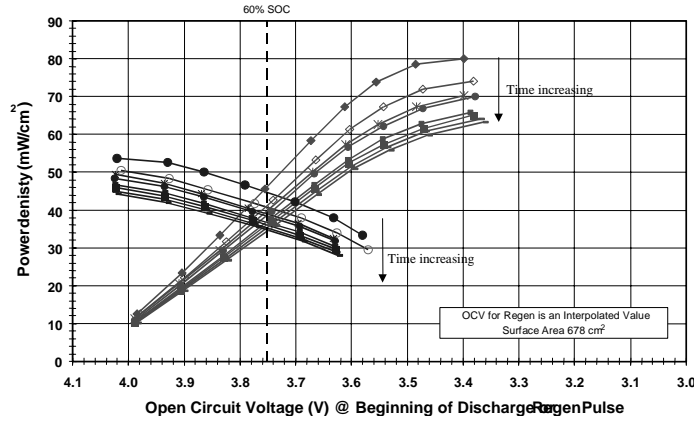
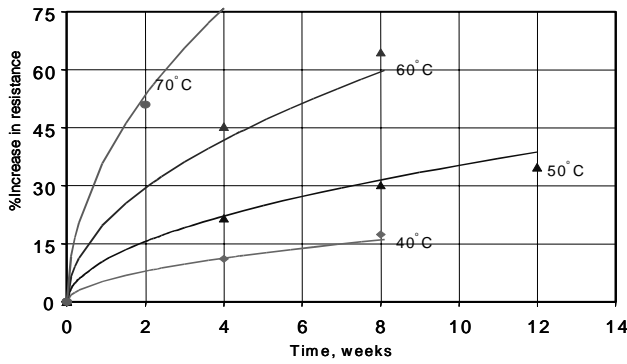
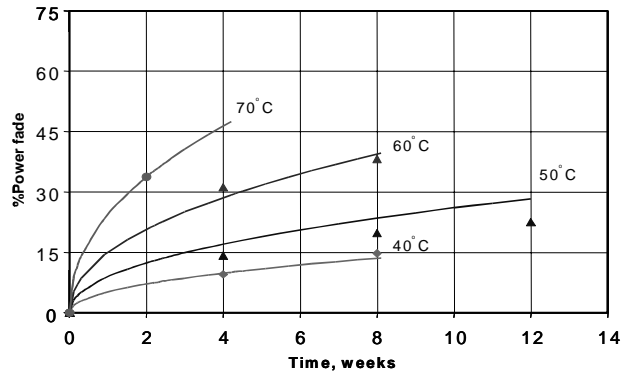


FIG. 4. Typical HPPC-derived power density vs. cell voltage curves.

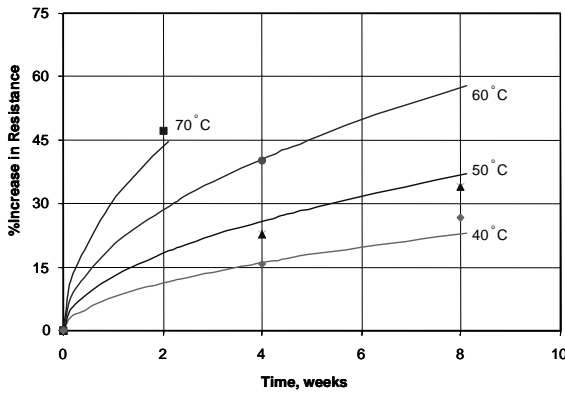


(a)

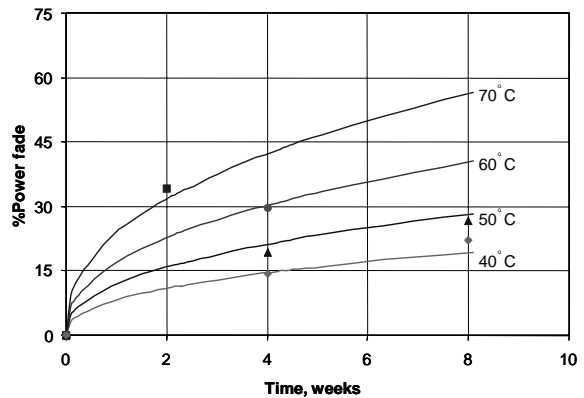


(b)

FIG. 5. (a) %Increase in resistance and (b) %power fade for Group A calendar life cells at 60% SOC. Markers represent the experimental values.



(a)



(b)

Fig. 6. (a) %Increase in resistance and (b) %power fade for Group B calendar life cells at 60% SOC. Markers represent the experimental values.

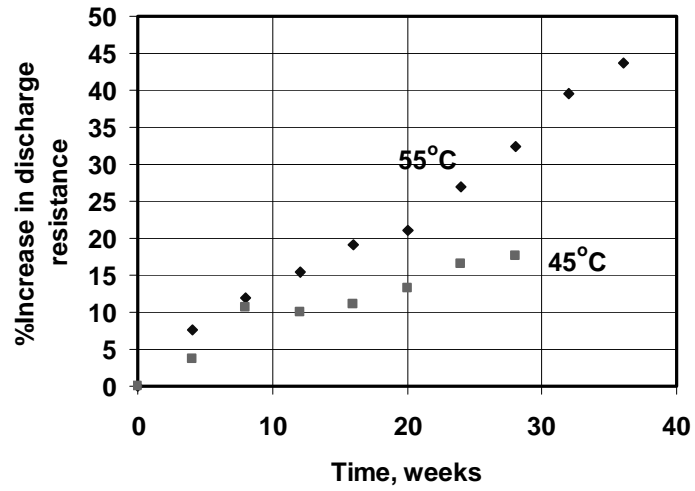


Fig. 7. Change in discharge resistance with time for Gen 2 calendar life test.

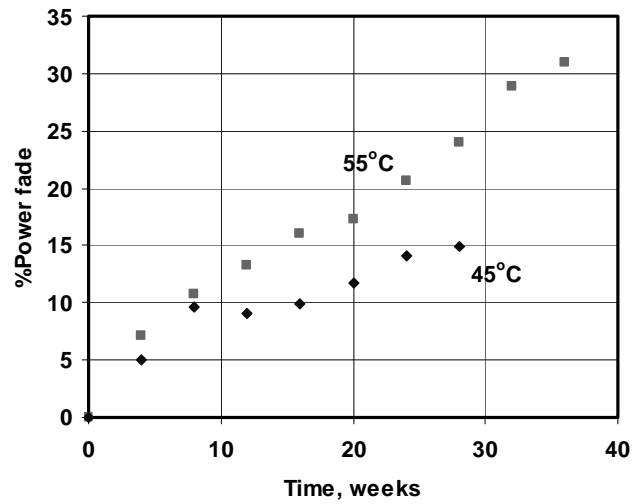


Fig. 8. Power fade with time for Gen 2 calendar life testing.

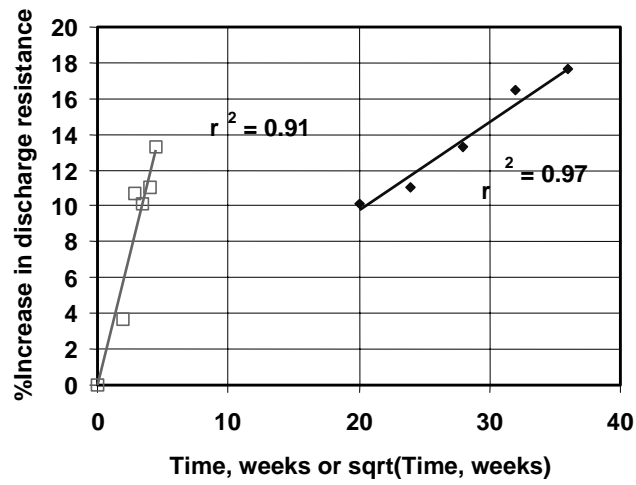


Fig. 9. %Increase in discharge resistance as functions of time at 45°C for Gen 2 calendar life testing.

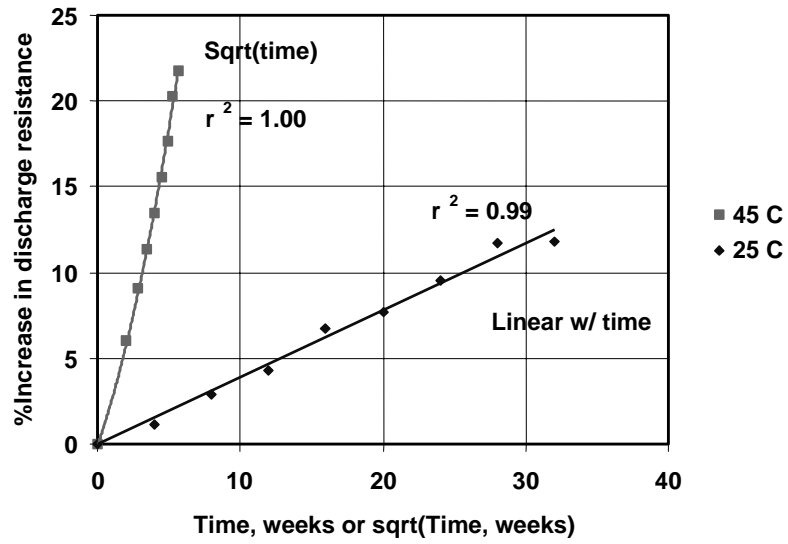


Fig. 10. %Increase in discharge resistance for Gen 2 cycle life cells.